Optical force and its applications based on heterosexual phosphorene waveguide

Chunyu Lu, Jicheng Wang, Zheng-Da Hu
School of Science
Jiangnan University
Wuxi 214122, China

Liang Pan
School of Mechanical Engineering and Birck
Nanotechnology Center
Purdue University
West Lafayette, Indiana 47907, USA

***Abstract*—We study the optical properties of face-to-face phosphorene pairs, including propagation length, optical constraint, and gradient force. The symmetric and anti-symmetric plasmonic modes occur on account of the strong anisotropic dispersion of phosphorene. Compared with the anti-symmetric mode, the symmetric mode owns stronger optical constraint and much larger gradient force. Based on the large gradient force and high optical constraint, we also propose a scheme of ultra-small phase shifter. Our results may suggest an opportunity for optical manipulation and development of photonic phosphorene-based devices.**

Keywords—phosphorene pairs; propagation length; light confinement; gradient force

I. INTRODUCTION

When light spreads in two parallel waveguides, the optical gradient force will be generated [1]. This force can be either attraction or repulsion. It depends on the relative phase difference of corresponding guided modes in the two waveguides, which is 0 or π [2]. This furnishes a new manner for manipulation of the light in photonic molectron [3-10]. To manipulate the light better, larger optical force is required [11-14]. People can enhance the optical force by employing slow light in photonic crystals [15], the cavity resonance of a high-Q (quality factor) optical resonator, metamaterials and surface plasmon polaritons (SPPs). As a result of the strong optical energy constraint of metallic surface plasmons (MSPs), the optical force can be enhanced substantially.

Lately, it is discovered that the graphene can support the formation and propagation of SPPs in infrared and terahertz ranges [16-24]. Furthermore, as a newly found 2D material, single-layer black phosphorus (BP), the so-called phosphorene, has attracted more and more research interest in recent years owing to its natural semi-conductor properties. In 2014, phosphorene was first synthesized from the bulk BP using a scotch-tape-based microcleavage [25]. Nevertheless, researches on the basic properties and potential applications of phosphorene are in the infancy. In phosphorene, the covalent bonds of the phosphorus atoms make a hexagonal lattice of a folded cellular structure with other three atoms [26]. This special atomic structure causes extremely anisotropic electronic dispersion and direction-dependent conductivity [27-29]. As a 2D material, a lot of researches have been done on graphene, and compared to graphene, phosphorene may be more suitable for series of applications, such as nano-resonators [30], flexible electronics [31], charge trap memories [32], Terahertz photodetection [33], and amplitude modulation (AM) demodulators [31].

In this paper, we set the two phosphorene layers in three different relative orientations, and the symmetric mode and of the anti-symmetric mode are found in all three configurations. Results show that the symmetric modes exhibit larger optical constraint and gradient force compared to the anti-symmetric modes in BP pairs. More interestingly, we find that the armchair-armchair configuration has the largest propagation length, the zigzag-zigzag configuration has the largest gradient force, while the armchair-zigzag has the largest optical constraint ratio. Compared with the relevant parallel silicon nanobeams, the anisotropy and the optical parameter of the black phosphorus which is related to the thickness provide more tenability to us. Our results may be of benefit to the implementation of nanoscale optical manipulation and facilities based on BP. Finally, we propose an application example of our results as an ultra-small phase shifter.

II. RESULTS AND DISCUSSIONS

We study the optical properties of separated and face-to-face phosphorene pairs. The gap d is sandwiched between the separated phosphorene pair. The width and the thickness of the phosphorene are respectively defined as w and t. Figure 1(a) shows the electric field y-components of the symmetric mode and of the anti-symmetric mode with d = 50 nm for the armchair direction. From Fig. 1(b), we can see the effective refractive index of the symmetric mode is larger than that of the anti-symmetric mode. Meanwhile, with the gap d increasing, the inclination of the former becomes larger, which indicates a larger optical field gradient. The propagation lengths ($1/[2|\mathrm{Im}(\beta)|]$) of the two modes are shown in Fig. 1(c).

Besides, we discuss the optical constraint ratio in the BP pair, which is specified as the ratio of the integrated Poynting

vector P_z in the regions between and outside the phosphorene layers,

$$\xi = \int_{-d/2}^{d/2} P_z \mathrm{d}s \Big/ \int_{-\infty}^{\infty} P_z \mathrm{d}s \quad (1)$$

The distributions of P_z in the BP structures can be obtained by using the FEM simulations, and the optical constraint ratio ξ can be obtained by integrating P_z vertical to the phosphorene layers.

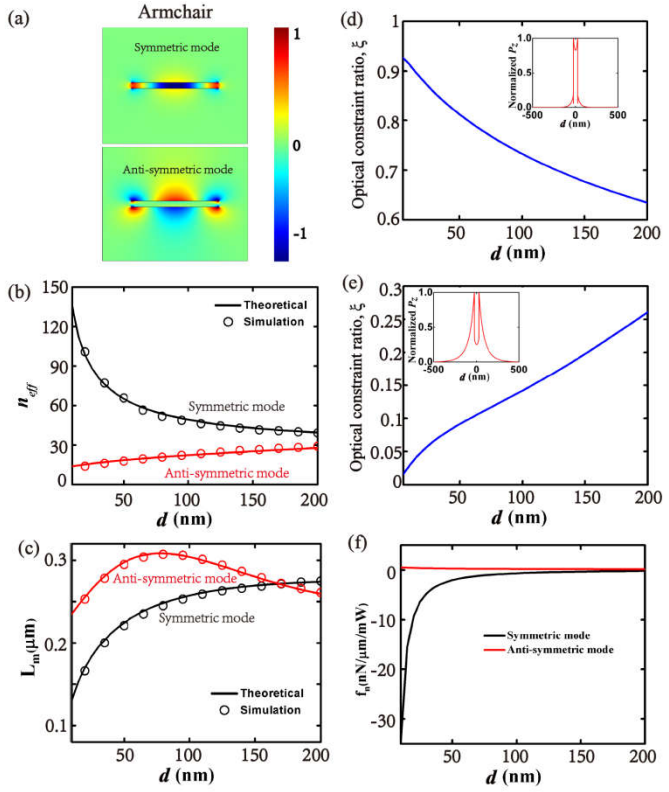

Fig. 1 (a-c) The electric field, effective refractive index, propagation length of the symmetric and anti-symmetric modes for the armchair direction. (d,e) Optical constraint ratio(ξ) of the two modes in the BP pair The inset shows the intensity of normalized P_z. (f) The gradient force of the two modes.

Through integrating the Maxwell Stress Tensor (MST) around a discretional surface containing the phosphorene pairs, and the gradient force f_n can be calculated [1]. By defining [26]

$$T_{ij} = \varepsilon_0 (E_i E_j - \delta_{ij} E^2/2) + \mu_0 (H_i H_j - \delta_{ij} H^2/2), \quad (2)$$

where δ is the Kronecker delta function, the normalized gradient force along y direction is defined as

$$f_n = \oint_S T \mathrm{d}S \cdot n_y, \quad (3)$$

where S is the surface of the volume containing the phosphorene pairs and n_y is the unit vector along the y direction.

Figures 1(d, e) respectively show the optical constraint ratio of the two modes. Just as the inset of Fig. 1(d), for the symmetric mode, most light power can be concentrated between the phosphorene pair, while the majority of the light power spreads outside of the BP pair for the anti-symmetric mode as the inset of Fig. 1(e) shows. The strong constraint of light in the waveguides makes the contribution to the formation of giant force [29]. Figure 1(f) shows the gradient force f_n as functions of the gap d for the two modes. It can be learnt that in comparison with the symmetric mode, the gradient force f_n under the anti-symmetric mode can even be ignored.

III. THE OPTOMECHANICAL APPLICATIONS

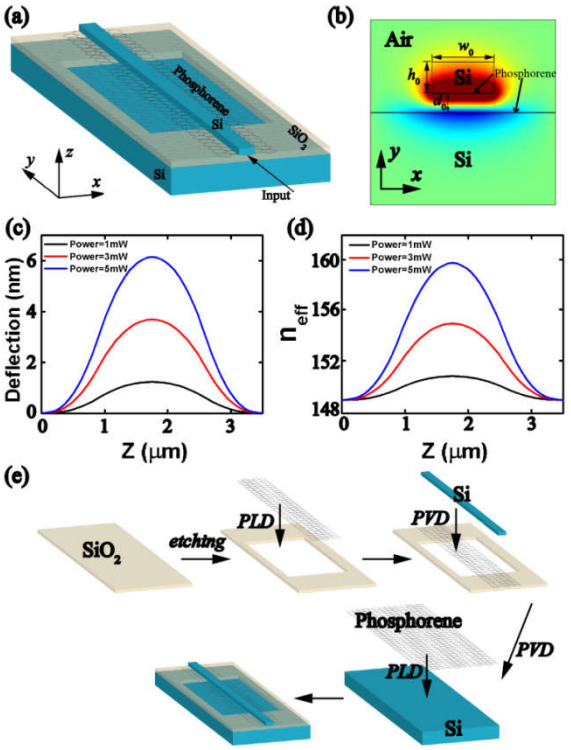

Fig. 2 (a) The 3D schematic illustration of the optomechanical phase shifter. (b) The electric field x-component at wavelength λ_0 = 10 μm. (c,d) Deflection and the effective refractive index along the free-standing waveguide under the circumstance of different incident power. (e) Schematic illustration of the fabrication procedures of the device.

In virtue of the strong gradient force between the phosphorene sheets, we propose a realization of untra-small phase shifter working in mid-infrared region. The 3D schematic illustration is shown in Fig. 2(a). Figure 2(b) shows the electric field. Both the phosphorene sheet and nanoribbon are set along the armchair direction. The deflection of the double-clamped beam is shown in Fig. 2(c). The separation of the phosphorene sheet and nanoribbon becomes narrower owing to the change of deflection, and causes the change of the effective refractive index as Fig. 2(d) shows. Figure 2(e) simply shows the fabrication procedures of the device.

Finally, we can obtain the phase shift resulting from different incident power with the following formula:

$$\Delta\varphi = \int \beta_1(z)\mathrm{d}z - \int \beta_2(z)\mathrm{d}z, \quad (4)$$

where $\Delta\varphi = k_0 \cdot S$ and S is the region sandwiched by two curves with propagation constants $\beta_1(z)$ and $\beta_2(z)$.

Acknowledgment

This work is supported by the National Natural Science Foundation of China (Grant Nos. 11504139, 11504140, 1171101387), National Science Foundation (NSF) (CMMI-1405078, CMMI-1554189, CMMI-1634832), the Natural Science Foundation of Jiangsu Province (Grant Nos. BK20140167, BK20140128), the China Postdoctoral Science Foundation (2017M611693), and the Open Fund of State Key Laboratory of Millimeter Waves (Grant No. K201802).

References

[1] J. D. Jackson, Classical Electrodynamics, 3 edn, 258–262 (1998).

[2] M. L. Povinelli, et al. "Evanescent-wave bonding between optical waveguides." Opt. Lett. 30, 3042–3044 (2005).

[3] M. Li, et al. "Harnessing optical forces in integrated photonic circuits." Nature 456, 480–484 (2008).

[4] J. Ma and M. L. Povinelli, "Large tuning of birefringence in two strip silicon waveguides via optomechanical motion." Opt. Express 17, 17818–17828 (2009).

[5] D. Van Thourhout and J. Roels, " Optomechanical device actuation through the optical gradient force." Nat Photon 4, 211–217 (2010).

[6] J. Ma and M. L. Povinelli, " Mechanical Kerr nonlinearities due to bipolar optical forces between deformable silicon waveguides." Opt. Express 19, 10102–10110 (2011).

[7] Z. Q. Wang, L. Shi, Y. Liu, X. B. Xu and X. L. Zhang, " Optical nonreciprocity in asymmetric optomechanical couplers." Sci. Rep. 5, 8657 (2015).

[8] X. D. Yang, Y. M. Liu, R. F. Oulton, X. B. Yin and X. Zhang, " Optical forces in hybrid plasmonic waveguides." Nano Lett. 11, 321 (2011).

[9] D. Palima and J. Glückstadm, "Gearing up for optical microrobotics: micromanipulation and actuation of synthetic microstructures by optical forces." Laser Photonics Rev. 7, 478-494 (2013).

[10] J. Youngho, S. Jaeho, K. Kyungmook, J. B. You, C. Kyunghan, and K. Yu, "Hybrid integration of III-V semiconductor lasers on silicon waveguides using optofluidic microbubble manipulation." Sci. Rep. 6, 29841 (2016).

[11] Y. E. Lee, O. D. Miller, M. T. Homer Reid, S. G. Johnson, and N. X, Fang, " Computational inverse design of non-intuitive illumination patterns to maximize optical force or torque." Opt. Express 25, 6757 (2017).

[12] T. R. Lin, C. H. Lin and J. C. Hsu, "Strong Optomechanical Interaction in Hybrid Plasmonic-Photonic Crystal Nanocavities with Surface Acoustic Waves." Sci. Rep. 5, 13782 (2015).

[13] R. Leijssen and E. Verhagen, " Strong optomechanical interactions in a sliced photonic crystal nanobeam." Sci. Rep. 5, 15974 (2015).

[14] C. W. Qiu, D. Palima, A. Novitsky, D. Gao, W. Ding, S. V. Zhukovsky, and J. Gluckstad, "Engineering light-matter interaction for emerging optical manipulation applications." Nanophotonics 3, 181-201 (2014).

[15] M. L. Povinelli, M. Ibanescu, S. G. Johnson and J. D. Joannopoulos, "Slow-light enhancement of radiation pressure in an omnidirectional-reflector waveguide." Appl. Phys. Lett. 85, 1466 (2004).

[16] L. Ju, B. Geng, J. Horng, C. Girit, M. Martin, Z. Hao, H. A. Bechtel, X. Liang, A. Zettl, Y. R. Shen, and F. Wang, "Graphene plasmonics for tunable terahertz metamaterials." Nat. Nanotechnol. 6, 630-634 (2011).

[17] A. Grigorenko, M. Polini, and K. Novoselov, "Graphene plasmonics." Nat. Photonics 6, 749-758 (2012).

[18] V. W. Brar, M. S. Jang, M. Sherrott, J. J. Lopez, and H. A. Atwater, "Highly Confined Tunable Mid-Infrared Plasmonics in Graphene Nanoresonators." Nano Lett. 13, 2541-2547 (2013).

[19] H. Cheng, S. Chen, P. Yu, X. Duan, B. Xie, and J. Tian, "Dynamically tunable plasmonically induced transparency in periodically patterned graphene nanostrips." Appl. Phys. Lett. 103, 203122 (2013).

[20] Q. Zhang, X. Li, M. M. Hossain, Y. Xue, J. Zhang, J. Song, J. Liu, M. D. Turner, S. Fan, Q. Bao, and M. Gu, "Graphene surface plasmons at the near-infrared optical regime." Sci. Rep. 4, 6559 (2014).

[21] A. Vakil, and N. Engheta, " Transformation optics using graphene." Science 332, 1291-1294 (2011).

[22] P. Alonso-González, A. Y. Nikitin, F. Golmar, A. Centeno, A. Pesquera, S. Vélez, J. Chen, G. Navickaite, F. Koppens, A. Zurutuza, F. Casanova, L. E. Hueso, and R. Hillenbrand, "Controlling graphene plasmons with resonant metal antennas and spatial conductivity patterns." Science 344, 1369-1373 (2014).

[23] A. Yu. Nikitin, P. Alonso-González, and R. Hillenbrand, "Efficient coupling of light to graphene plasmons by compressing surface polaritons with tapered bulk materials." Nano Lett. 14, 2896-2901 (2014).

[24] P. Y. Chen, and A. Alù, "Atomically thin surface cloak using graphene monolayers." ACS Nano 5, 5855-5863 (2011).

[25] H. Liu, A. T. Neal, Z. Zhu, Z. Luo, X. Xu, D. Tomanek and P. D. Ye, "Phosphorene: an unexplored 2D semiconductor with a high hole mobility." ACS Nano 8, 4033 (2014).

[26] L. Li, Y. Yu, G. J. Ye, Q. Ge, X. Ou, H. Wu, D. Feng, X. H. Chen and Y. Zhang, "Black Phosphorus Field-effect Transistors." Nat. Nanotechnol. 9, 372–377 (2014).

[27] S. Zhang, J. Yang, R. Xu, F. Wang, W. Li, M. Ghufran, Y. W. Zhang, Z. Yu, G. Zhang, Q. Qin and Y. Lu, "Extraordinary Photoluminescence and Strong Temperature/Angle-Dependent Raman Responses in Few-Layer Phosphorene." ACS Nano 8, 9590–9596 (2014).

[28] Z. Liu and K. Aydin, "Localized Surface Plasmons in Nanostructured Monolayer Black Phosphorus." Nano Lett. 16, 3457–3462 (2016).

[29] H. Lu, Y. Gong, D. Mao, X. Gan and J. Zhao, "Strong plasmonic confinement and optical force in phosphorene pairs." Opt. Express 25, 5255-5263 (2017).

[30] C. X. Wang, C. Zhang, J. W. Jiang, H. S. Park, T. Rabczuk, "Mechanical strain effects on black phosphorus nanoresonators." Nanoscale 8, 901–905 (2016).

[31] W. N. Zhu, M. N. Yogeesh, S. X. Yang, S. H. Aldave, J. S. Kim, S. Sonde, L. Tao, N. S. Lu and D. Akinwande, "Flexible black phosphorus ambipolar transistors, circuits and AM demodulator." Nano Lett. 15, 1883–1890 (2015).

[32] Q. Feng, F. G. Yan, W. G. Luo and K. Y. Wang, "Charge trap memory based on few-layer black phosphorus." Nanoscale 8, 2686–2692 (2016).

[33] L. Viti, J. Hu, D. Coquillat, W. Knap, A. Tredicucci, A. Politano and M. S. Vitiello, "Black phosphorus terahertz photodetectors." Adv. Mater. 27, 5567–5572 (2015).